Electronic Supplementary Information

A duplex connection can further illuminate G-quadruplex/crystal violet complex

Shuang Wang,[†,‡] Jiahui Zhao[†,§] Shasha Lu,[†,‡] Jian Sun,[†] and Xiurong Yang[†,‡,§ *]

† State Key Laboratory of Electroanalytical Chemistry, Changchun Institute of Applied Chemistry, Chinese Academy of Sciences, Changchun, Jilin 130022, China

‡ University of Science and Technology of China, Hefei, Anhui 230026, China

§ University of Chinese Academy of Sciences, Beijing 100049, China

*Corresponding author

Tel.: +86 431 85262056; Fax: +86 431 85689278. E-mail: xryang@ciac.ac.cn.

EXPERIMENTAL SECTION

Materials and reagents. All the DNA sequences listed in Table S1 were synthesized and purchased habitually by the Sangon Biotechnology Co., Ltd. (Shanghai, China). The DNAs were dissolved by 25 mM Tris-HCl (pH = 7.0, 100 mM KCl) and annealed within the PCR equipment by 95°C for 5 min and being cooled to room temperature at 6°C /min and then used after accurate quantification via measuring the UV-vis absorbance at 260 nm with the following extinction coefficients (ε) for each nucleotide: A = 15400, T = 8700, C = 7400, G = 11500. N-methyl mesoporphyrin IX (NMM) were purchased from Sigma-Aldrich (St Louis, MO). Crystal violet (CV) and methyl green (MEG) was purchased by Sangon Biotechnology Co., Ltd. (Shanghai, China) and dissolved with ultrapure water purified by Milli-Q water system with 18.25 MΩ cm. The human blood serum was supplied by The Second Hospital of Jilin University.

Live subject statement. All experiments were performed in accordance with the guidelines No. Yanshen 2014-016 and approved by the ethics committee at The Second Hospital of Jilin University. Study participants were fully informed regarding the purposes of the study and consent was obtained.

Instrumentations. CARY 500 UV-vis-NIR Varian spectrophotometer was employed to measure the UV-vis absorption spectra. Fluorescence spectra were performed on an F-4600 FL spectrophotometer (Hitachi, Japan) with excitation at 580 nm and emission ranging 600 nm to 700 nm. Jasco J-820 circular dichroism spectra polarimeter (Tokyo, Japan) was used to obtained circular dichroism spectra of different samples via averaging three results. The fluorescence lifetimes were measured with Horiba-Jobin-Yvon Fluorolog-3 spectrofluorometer (NJ, U.S.A.) with the time-correlated single-photon counting unit.

Density functional theory (DFT) calculation. Computational studies are performed with the Gaussian 09 software package. The ground geometry of CV was optimized at the DFT B3LYP/6-311G(d) level, followed by harmonic frequency calculations at the same level. The excited-state geometry of CV was obtained by TD-DFT calculations at the B3LYP/6-311G(d) level. The

dimensional plots of electron density for ground and excited states were generated with the GaussView program. The coordinates of optimized ground and excited state geometry of CV were displayed in Table S2-S3 of supporting information.

Process of bioanalysis. All characterizations including fluorescence spectra, CD and UV-vis absorbance spectra were implemented in 25 mM Tris-HCl (pH = 7.0, 100 mM KCl) solution. The different samples used for bioanalysis were prepared as follows: first, 5 μM probes (with different length or sequence types) reacted with corresponding complementary strands with different concentrations for 1 h at 37℃; then 10 μM CV was put in and interacted for another 1 h at room temperature; subsequently, the respective fluorescence signals of the mixture were recorded.

DNA detection in human serum. 1% human blood serum sample was obtained by diluting with 25 mM Tris−HCl (pH 7.0, 100 mM NaCl). DNA with different concentrations were added to the diluted human blood serum as mimic real sample and then incubated with 5 μM T-H for 1 h at 37℃. Subsequently, 10 μM CV was added to react with above mixture for 1 h at room temperature. Finally, the fluorescence spectra were measured. The concentrations obtained from experiments were compared with the added concentration.

Table S1. All the sequences used in our experiments

Primer	5'to3'
Hum 21 (H)	GGGTTAGGGTTAGGGTTAGGG
T_6-H	TTTTTTGGGTTAGGGTTAGGGTTAGGG
T_{10}-H	TTTTTTTTTTGGGTTAGGGTTAGGGTTAGGG
T_{16}-H	TTTTTTTTTTTTTTTTGGGTTAGGGTTAGGGTTAGGG
T_{22}-H	TTTTTTTTTTTTTTTTTTTTTTGGGTTAGGGTTAGGGTTAGGG
T_{28}-H	TTTTTTTTTTTTTTTTTTTTTTTTTTTTGGGTTAGGGTTAGGGTTAGGG
T_{34}-H	TTTTTTTTTTTTTTTTTTTTTTTTTTTTTTTTTTGGGTTAGGGTTAGGGTTAGGG
T_{40}-H	TTTTTTTTTTTTTTTTTTTTTTTTTTTTTTTTTTTTTTTTGGGTTAGGGTTAGGGTTAGG G
A_4	AAAA
A_{10}	AAAAAAAAAA
A_{16}	AAAAAAAAAAAAAAAA
A_{22}	AAAAAAAAAAAAAAAAAAAAAA
A_{28}	AAAAAAAAAAAAAAAAAAAAAAAAAAAA
A_{34}	AAAAAAAAAAAAAAAAAAAAAAAAAAAAAAAAAA
A_{40}	AAAAAAAAAAAAAAAAAAAAAAAAAAAAAAAAAAAAAAAA
A_4-H	AAAAttGGGTTAGGGTTAGGGTTAGGG
C_4-H	CCCCttGGGTTAGGGTTAGGGTTAGGG
G_4-H	GGGGttGGGTTAGGGTTAGGGTTAGGG
T_4	TTTT
C_4	CCCC
G_4(5.5G_4[a])	GGGG
A_{22}-H	AAAAAAAAAAAAAAAAAAAAAAGGGTTAGGGTTAGGGTTAGGG

T_{22}-H	TTTTTTTTTTTTTTTTTTTTTGGGTTAGGGTTAGGGTTAGGG
C_{22}-H	CCCCCCCCCCCCCCCCCCCCCCGGGTTAGGGTTAGGGTTAGGG
T_{22}	TTTTTTTTTTTTTTTTTTTTT
A_{22}	AAAAAAAAAAAAAAAAAAAAA
Probe 1	ACGGGTGCGATTTCTGTGTGAGAGGGTTAGGGTTAGGGTTAGGG
Probe 2 (T-H)	CCCCTCTGGTCAACCAGTCACAGGGTTAGGGTTAGGGTTAGGG
Probe 3	TTCAAAACATGAATTGCTGCTGGGGTTAGGGTTAGGGTTAGGG
Probe 4	CTTCCAGTCAAGGATGTTTACAGGGTTAGGGTTAGGGTTAGGG
$C_{Probe\ 1}$	TCTCACACAGAAATCGCACCCGT
$C_{Probe\ 2}$ (T)	TGTGACTGGTTGACCAGAGGGG
$C_{Probe\ 3}$	CAGCAGCAATTCATGTTTTGAA
$C_{Probe\ 4}$	TGTAAACATCCTTGACTGGAAG
T-H	CCCCTCTGGTCAACCAGTCACAGGGTTAGGGTTAGGGTTAGGG
C1	ATCGTGTAGCTGACATGCCTG
C2	GCTGATCTGAGCTAAAGCTAA
C3	AAAGGTTCCCATGACTAGGTT
C4	TTGACTTAGCTTAGCATCAAC
C5	GTAAAGGTCCATGGTATCGCT
C6	TTTCAGTTATATGGATGATGT
C7	TAGAGATTTTCCACACTGACT

[a]: 5.5 represents molar ratio of G4 to C22-H.

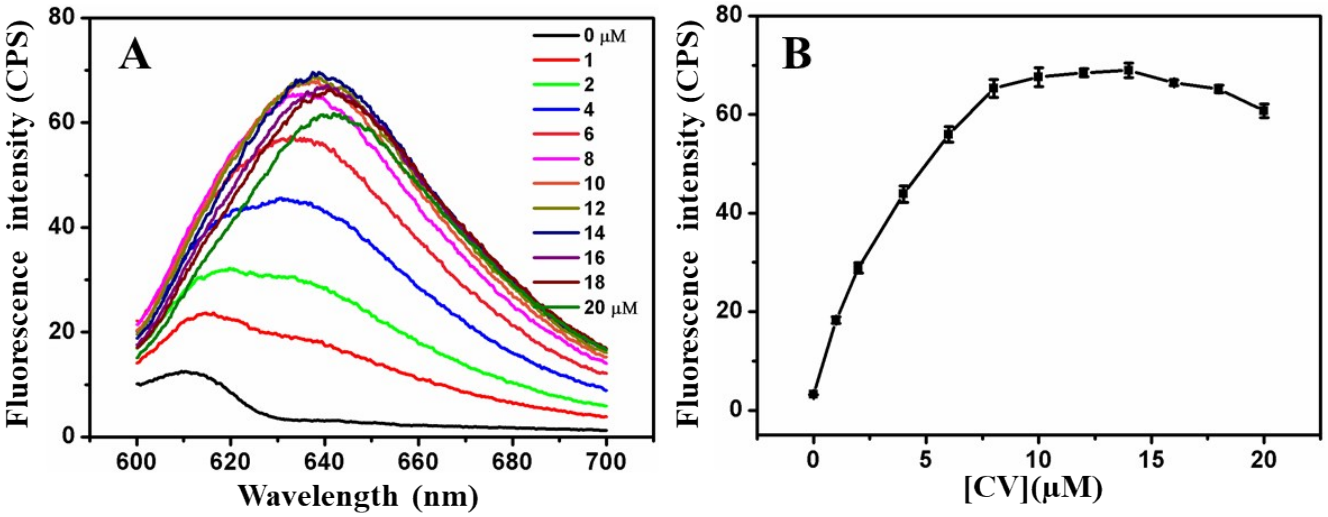

Fig. S1. Fluorescence spectra (A) and intensity (B) of H with increased CV ranging from 0 to 20 μM. The concentration of H was 5 μM.

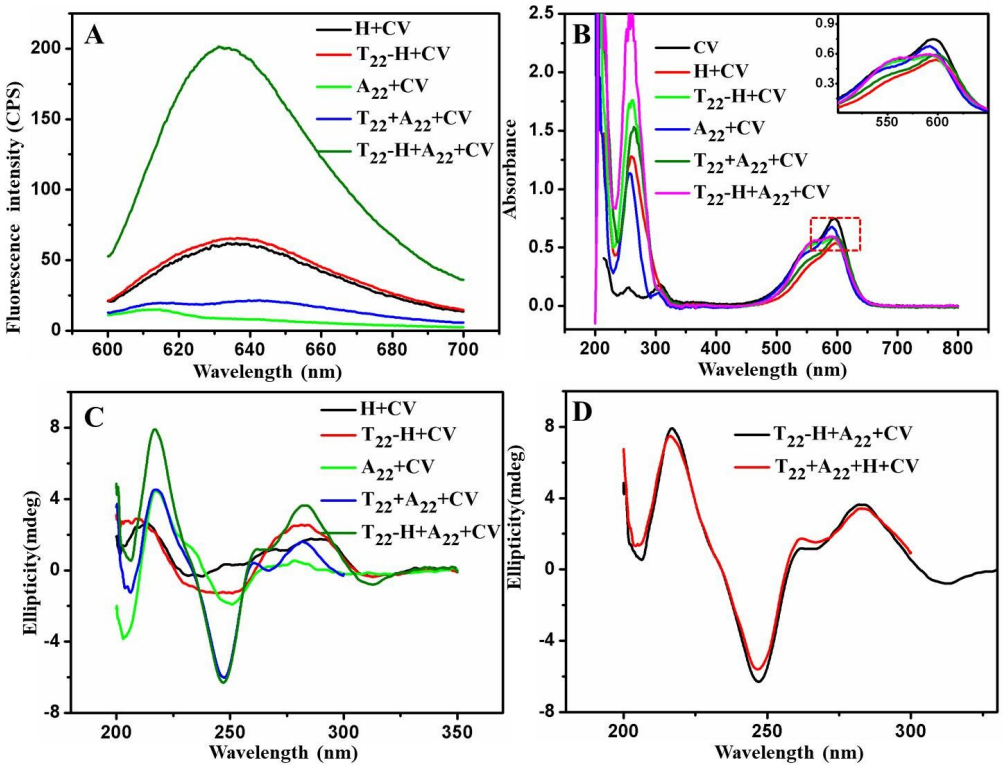

Fig. S2. Fluorescence (A), UV-vis (B) and circular dichroism (C) spectra of control sequences including H, T_{22}-H, A_{22}, A_{22} + T_{22}, T_{22}-H + A_{22} after binding CV. (D) Circular dichroism spectra of T_{22}-H + A_{22} and T_{22} + A_{22} + H. The concentrations of DNAs and CV were 5 μM and 10 μM.

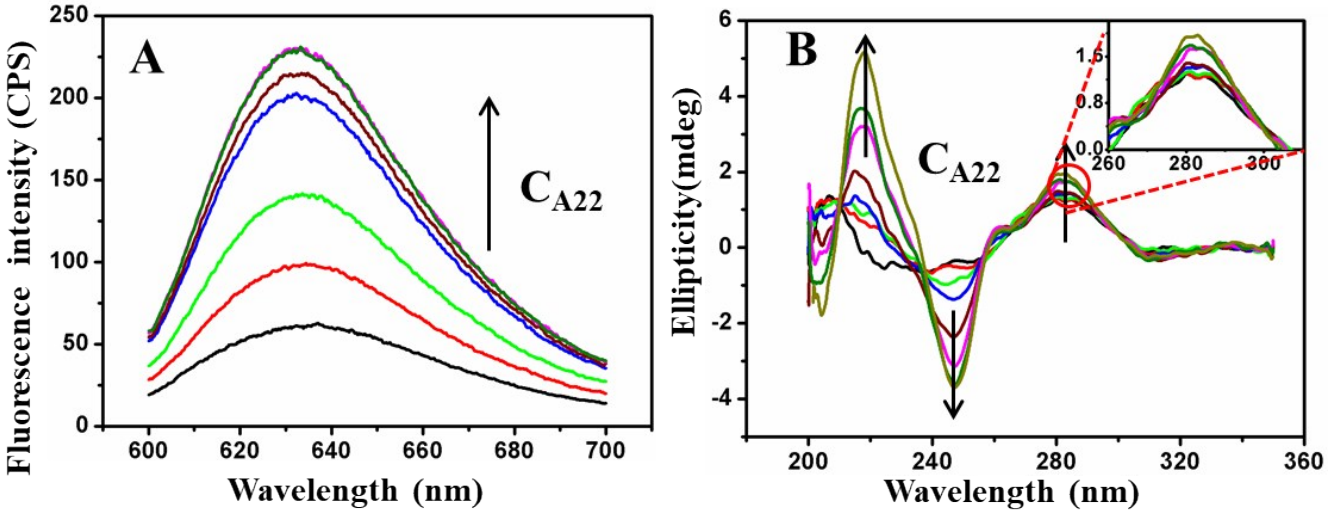

Fig. S3. Fluorescent spectra (A) and circular dichroism (B) of T_{22}-H in presence of increased complementary strand A_{22} ranging from 0 to 5 μM. The concentration of T_{22}-H and CV was 5 μM, 10 μM.

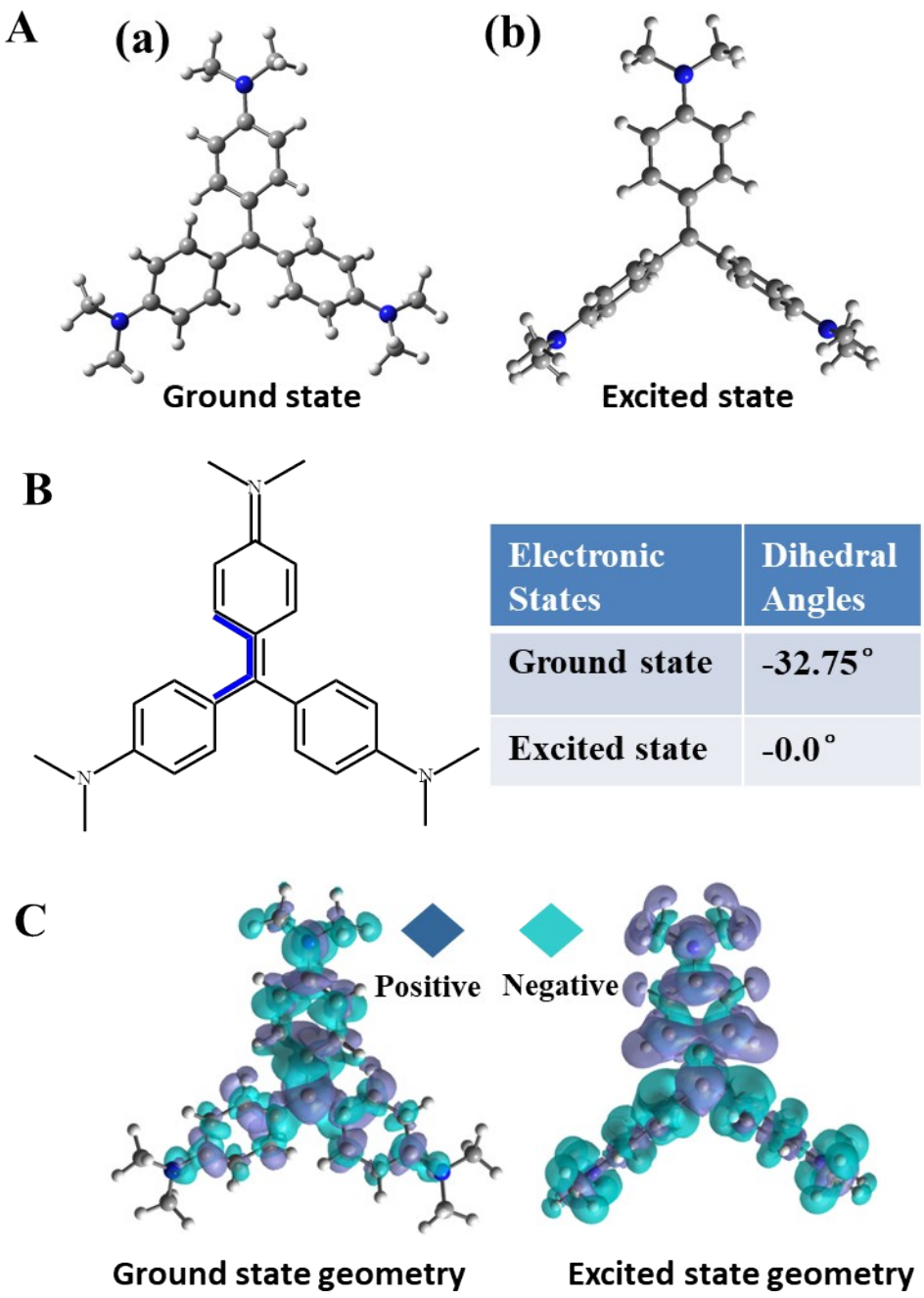

Fig. S4 (A) The optimized geometries of CV in ground state (a) and excited state (b). (B) A dihedral angle analysis confirmed structures of CV in both ground state (GS) and excited state (ES). (C) Charge density difference isosurfaces at the minimum energy conical intersection between ground state and excited state. Positive isosurfaces are blue and indicate electron withdraw. Negative isosurfaces are cyan and indicate electron donation.

Table S2. The optimized ground state geometry of CV.

Atom	X	Y	Z
C	1.0122	3.5664	0.67
C	1.0137	2.1916	0.652
C	0	1.4433	0
C	-1.0137	2.1916	-0.652
C	-1.0122	3.5664	-0.67
C	0	4.3104	0
H	1.7861	1.6656	1.2008
H	-1.7861	1.6656	-1.2008
H	-1.7893	4.0778	-1.2212
C	0	0	0
C	-1.25	-0.7217	0
C	-1.3911	-1.9737	-0.652
C	-2.4048	-0.2179	0.652
C	-2.5825	-2.6597	-0.67
H	-0.5495	-2.3796	-1.2008
C	-3.5946	-0.9066	0.67
H	-2.3355	0.7139	1.2008
C	-3.7329	-2.1552	0
H	-4.4261	-0.4894	1.2212
C	1.25	-0.7217	0
C	2.4048	-0.2179	-0.652
C	1.3911	-1.9737	0.652
C	3.5946	-0.9066	-0.67

H	2.3355	0.7139	-1.2008
C	2.5825	-2.6597	0.67
H	0.5495	-2.3796	1.2008
C	3.7329	-2.1552	0
H	4.4261	-0.4894	-1.2212
H	2.6369	-3.5885	1.2212
N	4.9097	-2.8346	0
H	-2.6369	-3.5885	-1.2212
N	-4.9097	-2.8346	0
H	1.7893	4.0778	1.2212
N	0	5.6692	0
C	1.0667	6.4109	0.6672
H	2.0474	6.1642	0.2497
H	0.9028	7.4763	0.5281
H	1.0849	6.2101	1.743
C	-1.0667	6.4109	-0.6672
H	-1.0849	6.2101	-1.743
H	-2.0474	6.1642	-0.2497
H	-0.9028	7.4763	-0.5281
C	-5.0186	-4.1292	-0.6672
H	-6.0232	-4.52	-0.5281
H	-4.8357	-4.0446	-1.743
H	-4.3146	-4.8552	-0.2497
C	-6.0853	-2.2816	0.6672
H	-5.9205	-2.1655	1.743

H	-6.362	-1.309	0.2497
H	-6.926	-2.9563	0.5281
C	6.0853	-2.2816	-0.6672
H	6.362	-1.309	-0.2497
H	6.926	-2.9563	-0.5281
H	5.9205	-2.1655	-1.743
C	5.0186	-4.1292	0.6672
H	4.8357	-4.0446	1.743
H	4.3146	-4.8552	0.2497
H	6.0232	-4.52	0.5281

Table S3. The optimized excited state geometry of CV.

C	0	1.2122	3.7979
C	0	1.2133	2.4275
C	0	0	1.6562
C	0	-1.2133	2.4275
C	0	-1.2122	3.7979
C	0	0	4.5452
H	0	2.1651	1.9099
H	0	-2.1651	1.9099
H	0	-2.164	4.3127
C	0	0	0.2694

C	0	-1.2227	-0.5885
C	-1.201	-1.807	-1.0356
C	1.201	-1.807	-1.0356
C	-1.2151	-2.9168	-1.8553
H	-2.1459	-1.3858	-0.7097
C	1.2151	-2.9168	-1.8553
H	2.1459	-1.3858	-0.7097
C	0	-3.5091	-2.2949
H	2.167	-3.3346	-2.1531
C	0	1.2227	-0.5885
C	-1.201	1.807	-1.0356
C	1.201	1.807	-1.0356
C	-1.2151	2.9168	-1.8553
H	-2.1459	1.3858	-0.7097
C	1.2151	2.9168	-1.8553
H	2.1459	1.3858	-0.7097
C	0	3.5091	-2.2949
H	-2.167	3.3346	-2.1531
H	2.167	3.3346	-2.1531
N	0	4.609	-3.1073
H	-2.167	-3.3346	-2.1531
N	0	-4.609	-3.1073
H	0	2.164	4.3127
N	0	0	5.9147
C	0	1.2559	6.6522

H	-0.8879	1.8563	6.4279
H	0	1.046	7.7189
H	0.8879	1.8563	6.4279
C	0	-1.2559	6.6522
H	-0.8879	-1.8563	6.4279
H	0.8879	-1.8563	6.4279
H	0	-1.046	7.7189
C	-1.2564	-5.2025	-3.5544
H	-1.0437	-6.0665	-4.1778
H	-1.8611	-5.5361	-2.7064
H	-1.8441	-4.4928	-4.1441
C	1.2564	-5.2025	-3.5544
H	1.8441	-4.4928	-4.1441
H	1.8611	-5.5361	-2.7064
H	1.0437	-6.0665	-4.1778
C	-1.2564	5.2025	-3.5544
H	-1.8611	5.5361	-2.7064
H	-1.0437	6.0665	-4.1778
H	-1.8441	4.4928	-4.1441
C	1.2564	5.2025	-3.5544
H	1.8611	5.5361	-2.7064
H	1.8441	4.4928	-4.1441
H	1.0437	6.0665	-4.1778

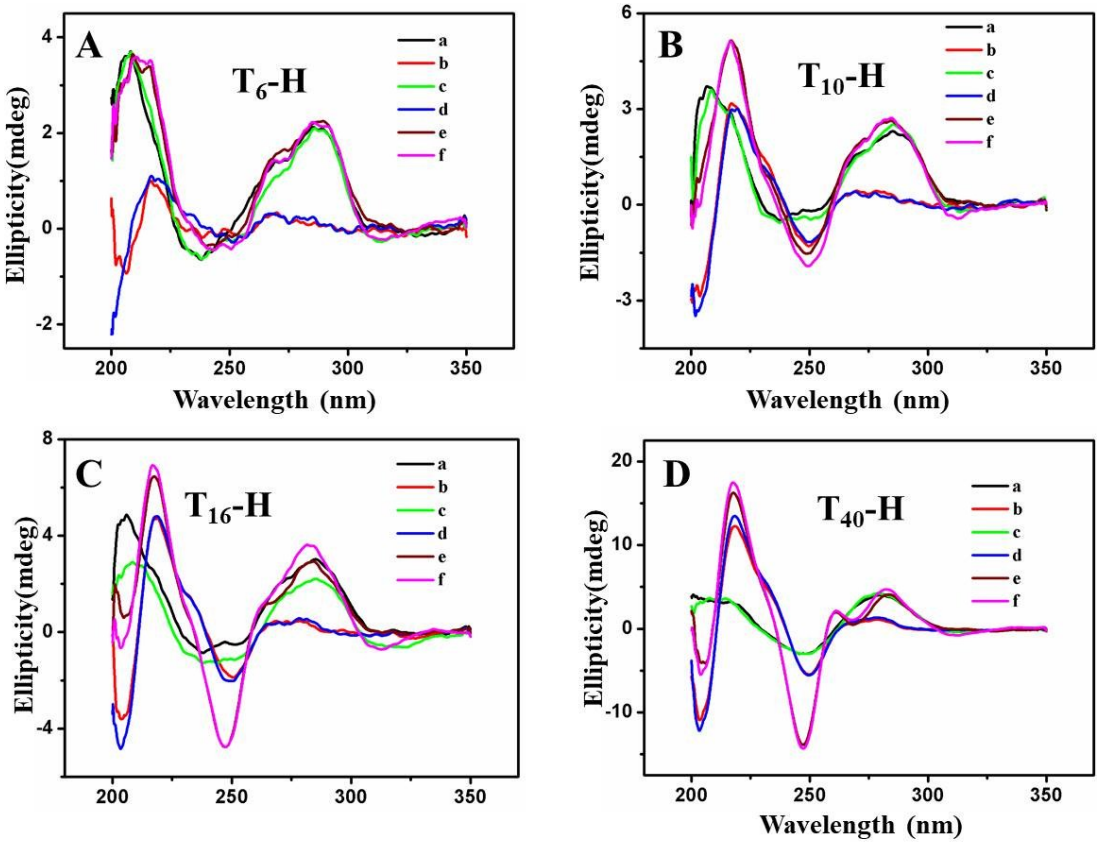

Fig. S5 Circular dichroism of Tx-H (a); Ax (b); Tx-H + CV (c); Ax + CV (d); Tx-H + Ax (e); Tx-H + Ax + CV (f). (A) x=4, (B) x=10, (C) x=16, (D) x=40. The concentration of probes, complementary strand and CV were 5 μM, 5 μM, and 10 μM, respectively.

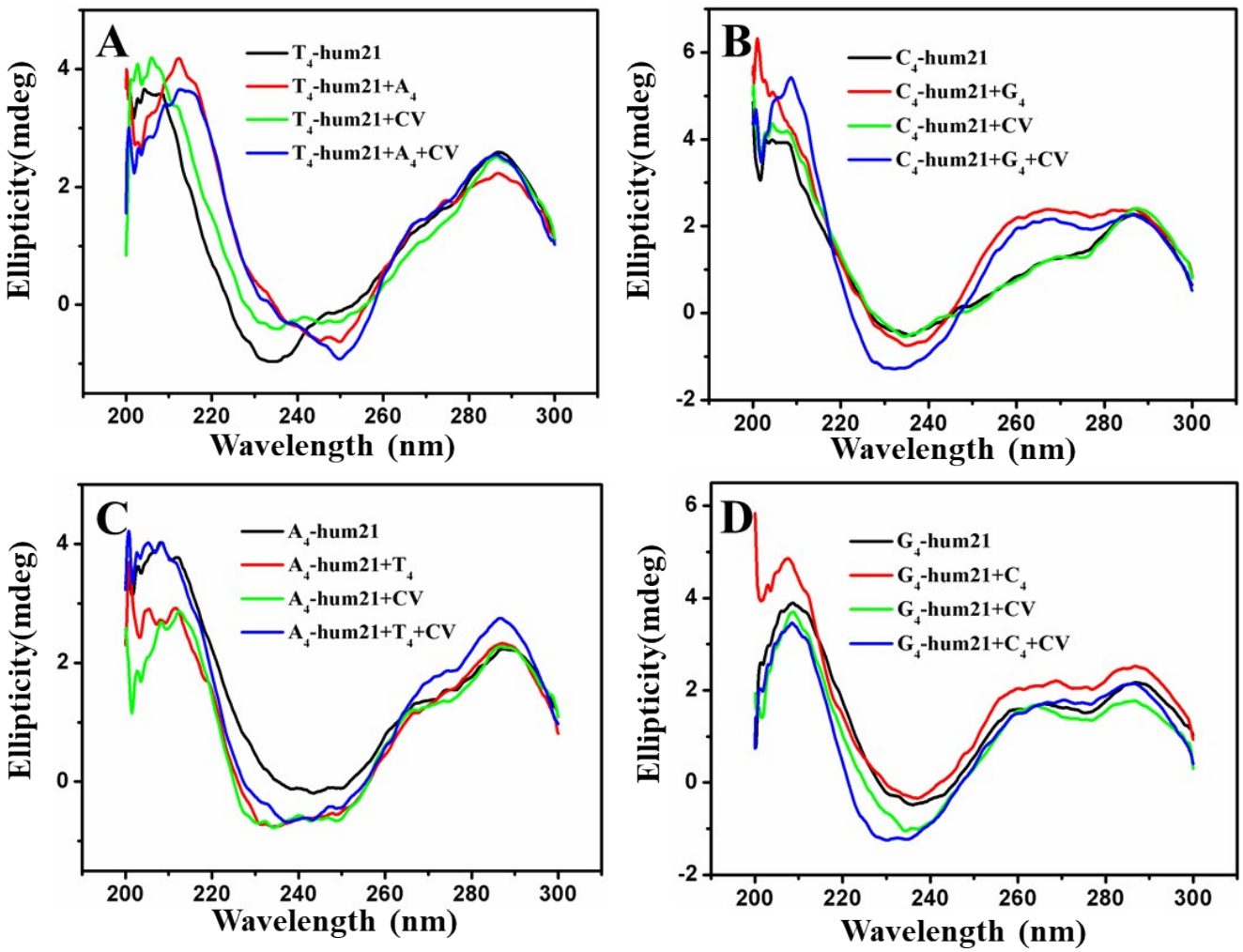

Fig. S6 Effect of bases types on the conformation of N_4-H in presence of corresponding complementary strands, CV and both of them. (A) N=T, (B) N=C, (C) N=A, (D) N=G. The concentration of probes, complementary strand and CV were 5 μM, 5 μM, and 10 μM, respectively.

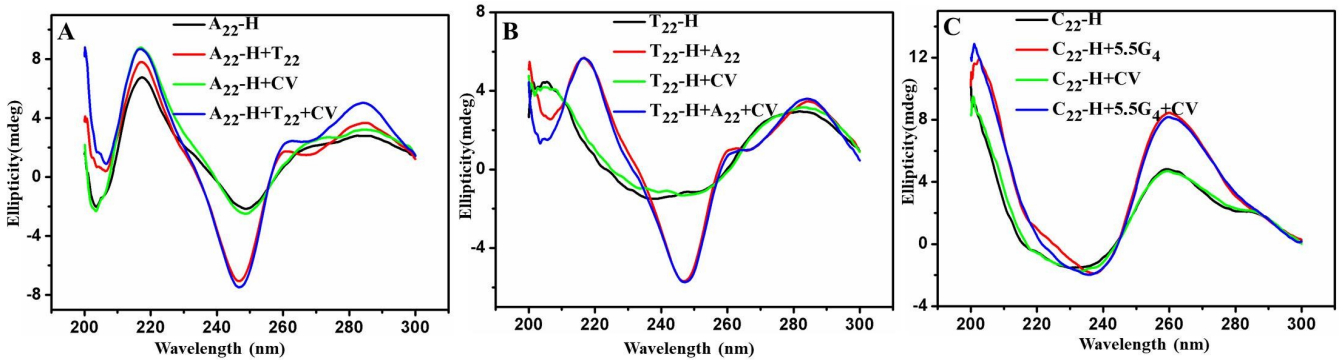

Fig. S7 Effect of bases types on the conformation of N_{22}-H in presence of corresponding complementary strands, CV and both of them. (A) N=A, (B) N=T, (C) N=C. The concentration of probes, complementary strand and CV were 5 μM, 5 μM, and 10 μM, respectively.

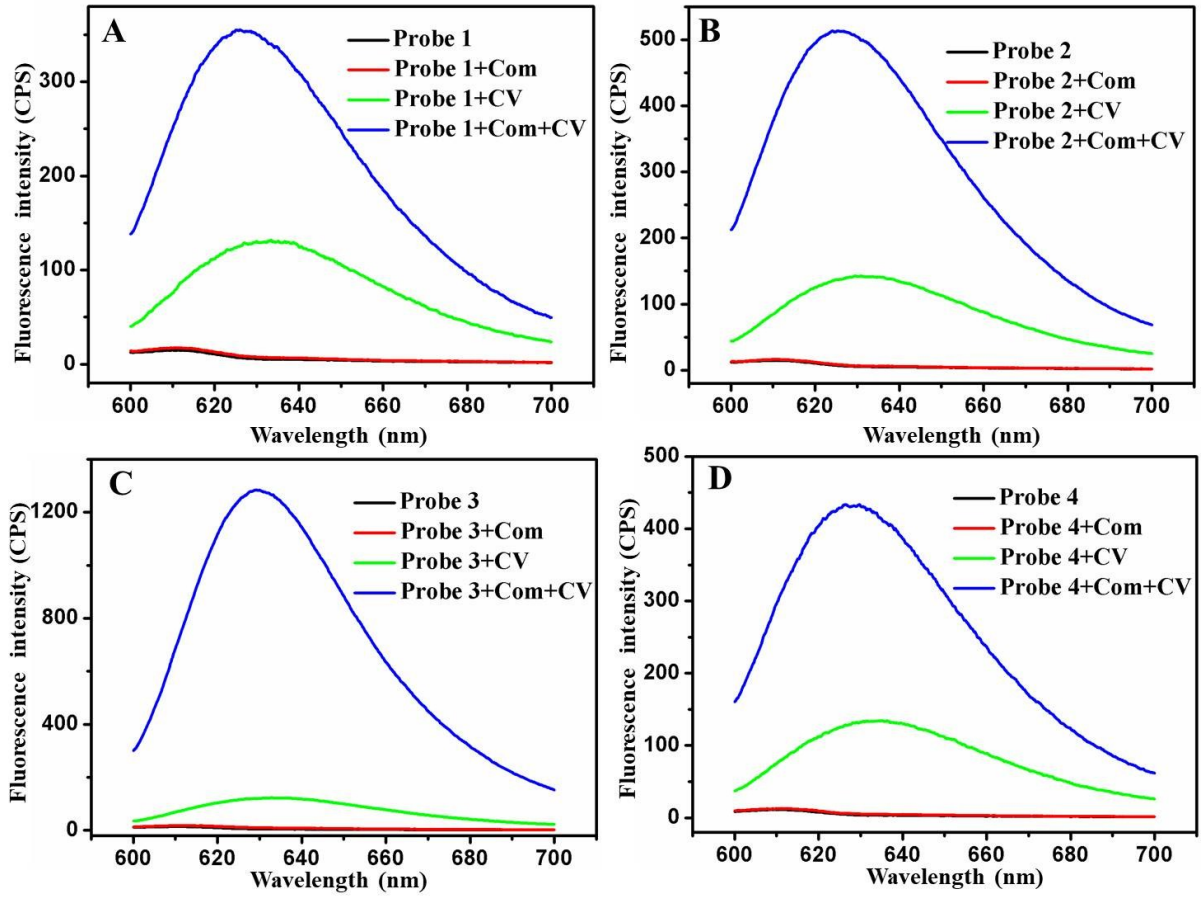

Fig. S8 Universality of duplex connection increased the fluorescence via substituting T_{22} with other DNA sequences shown in Probe 1 (A), Probe 2 (B), Probe 3 (C) and Probe 4 (D). The concentration of probes, complementary strand and CV were 4 μM, 4 μM, and 8 μM, respectively.

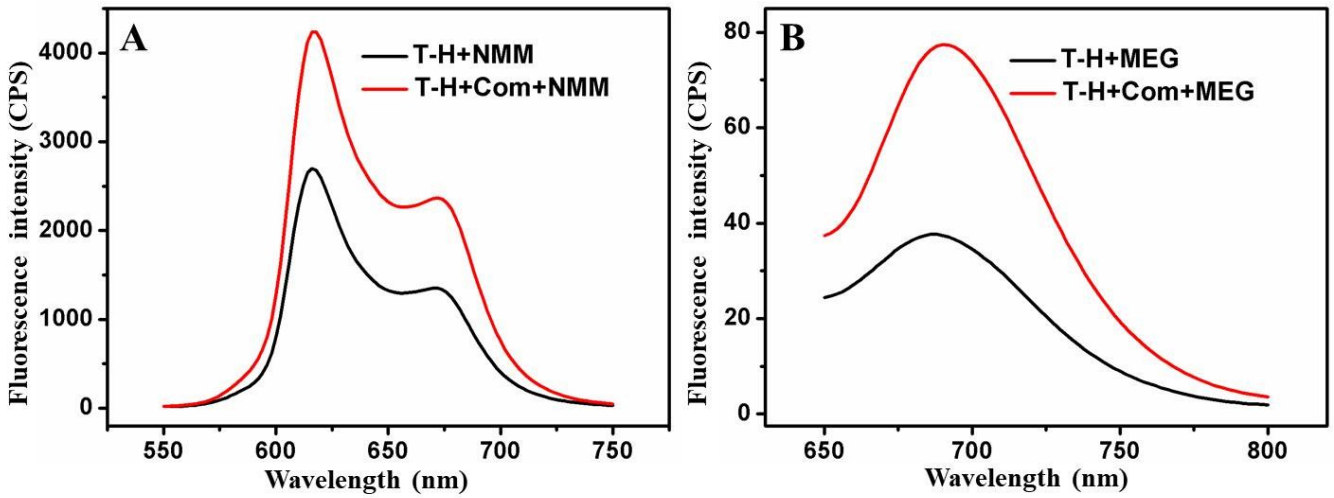

Fig. S9 Fluorescence spectra of T-H binding with NMM (A) and MEG (B) in absence (black line) and presence (red line) of the complementary stands. The concentration of probes, complementary strands, NMM and MEG were 4 μM, 4 μM, 8 μM and 8 μM, respectively.

Table S4. DNA detection in 1% human serum sample.

Samples	Spiked (μM)	Found (μM)	Recovery (%)	RSD (n=3.%)
1	0	-	-	-
2	0.200	0.213	1.06	4.67
3	0.500	0.498	0.996	3.55
4	2.00	2.12	1.06	3.46
5	4.00	4.04	1.01	5.58